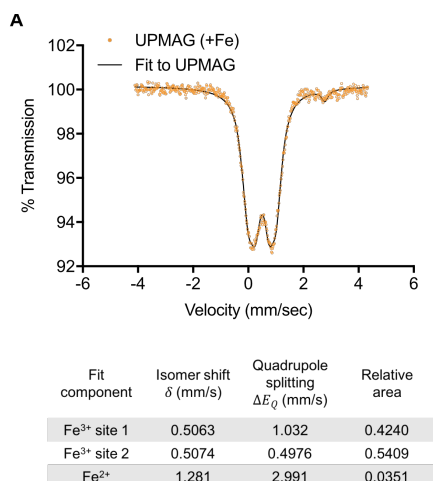


## SUPPLEMENTARY TABLES AND FIGURES

**Supplementary Table 1 – Measured and Theoretically Available Magnetic Susceptibility**

Genetic Construct	Measured Susceptibility $\Delta\chi_{\text{measured}}$	Intracellular Iron Concentration (fg/cell)	Theoretically Available Susceptibility $\Delta\chi_{\text{max}}$	Magnetic Efficiency ( $\Delta\chi_{\text{measured}}/\Delta\chi_{\text{max}}$ )
UPMAG	$4.68 \times 10^{-6}$	3.33	$9.24 \times 10^{-6}$	50.7%
BFR	$0.61 \times 10^{-6}$	1.89	$5.29 \times 10^{-6}$	11.5%

This table lists the measured magnetic susceptibility and iron contents of UPMAG and BFR cells (from Figure 2 of the main text), together with the theoretically available susceptibility assuming all the cellular iron is in a high spin state ( $S=5/2$ ). The last column lists the “Magnetic Efficiency” of the construct, defined as the fraction of the maximally available susceptibility it provides.



**Figure S1 | A.** Mössbauer spectroscopy of UPMAG *E. coli* at 80K. The three component fit parameters are listed in the table below the spectrum.

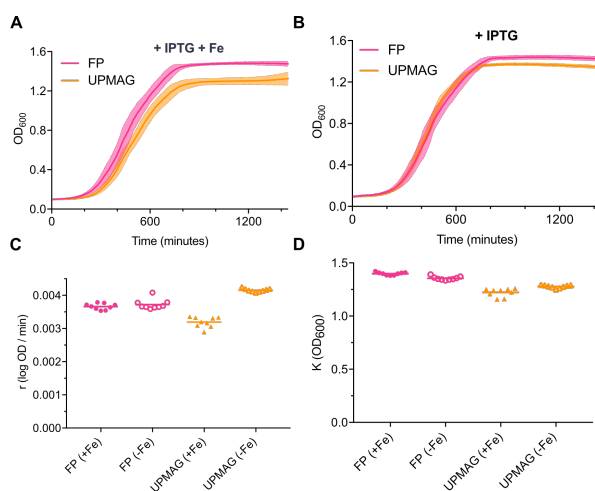


**Figure S2 | A.** Growth curves for *E. coli* expressing either FP or UPMAG in the presence of both inducer (0.1 mM IPTG) and iron (1 mM Fe(II)). **B.** Growth curves for *E. coli* expressing either FP or UPMAG in the presence of inducer (0.1 mM IPTG) alone **C.** Growth rates were obtained by fitting the modified Gompertz equation for the various conditions described in the text. **D.** Saturation OD as extracted from fits of the growth curves to the modified Gompertz equation.

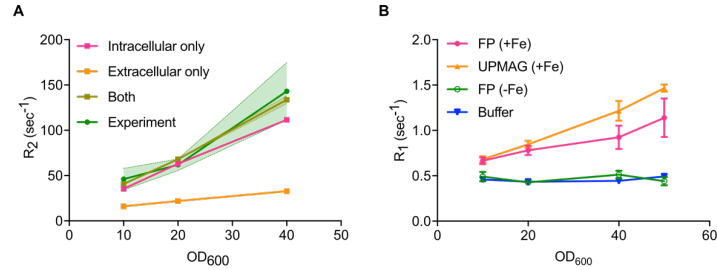


**Figure S3 | A.** Simulated transverse relaxation rates ( $R_2$ ) for UPMAG expressing *E. coli* for different cell densities. Exchange of water between compartments with a difference of + 4.68 ppm in bulk susceptibility accounts for the bulk of the observed transverse relaxation rates. **B.** Spin-lattice relaxation rates ( $R_1$ ) for *E. coli* expressing either FP or UPMAG grown under various conditions.

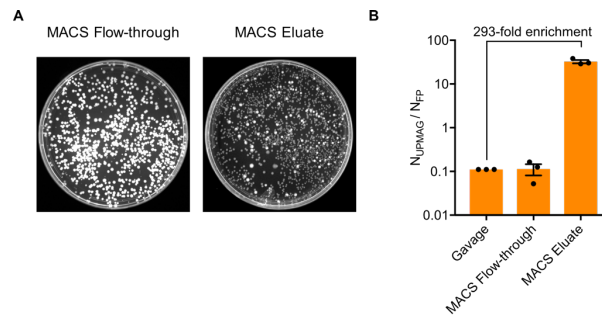


**Figure S4 | A.** Representative image of plates containing the flow-through and eluted fractions. **B.** Ratio of UPMAG to FP cells in the respective MACS fractions. UPMAG *E. coli* were enriched  $293 \pm 45.0$  fold in the MACS eluate.

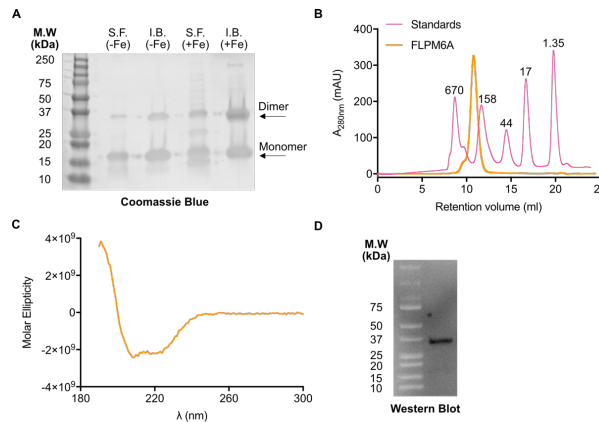


**Figure S5 | A.** SDS-PAGE of purified 6xHis-FLPM6A from the soluble and inclusion body fractions when cells were cultured either with or without iron. The I.B. (-Fe) and S.F. (+Fe) fractions were concentrated 5 fold prior to SDS-PAGE. The monomer and dimer molecular weights are 16 and 32 kDa respectively. **B.** Size-exclusion of FLPM6A purified from *E. coli* BL21 DE3. The molecular weights of standards are indicated above their respective peaks in the chromatogram. **C.** Circular Dichroism spectroscopy of purified FLPM6A **D.** Western Blot of purified FLPM6A which indicates a dimer.

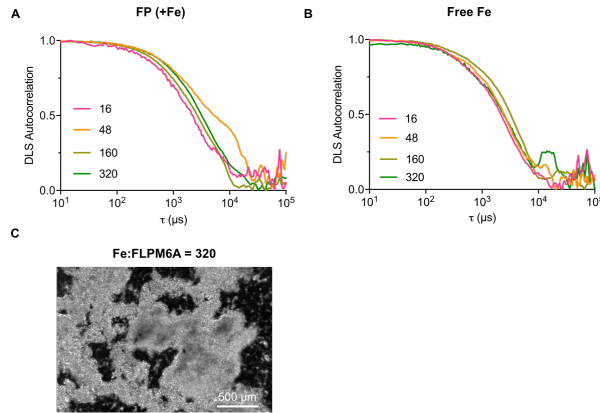


**Figure S6 | A.** DLS spectra for a hexa-histidine tagged fluorescent protein that was incubated with iron at varying molar ratios **B.** DLS spectra for equivalent concentrations of free iron **C.** Brightfield images of the “ferrogel”. FLPM6A was mixed with free iron at a ratio of 1:320 respectively in a glass bottom petri-dish. Unlike free iron which precipitates to the bottom of the dish, the ferrogel floats and no precipitates of iron were observed at the bottom when FLPM6A was present.

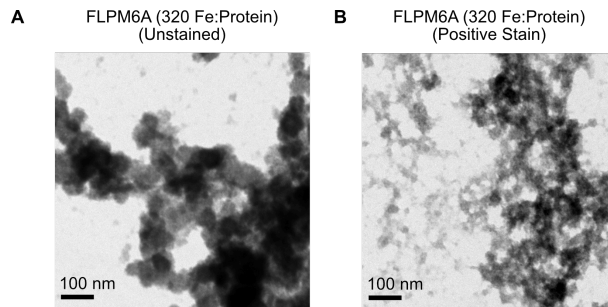


**Figure S7 | A.** Unstained TEM of FLPM6A incubated with 320 Fe:FLPM6A **B.** Positive stained TEM of the same sample indicating the presence of protein in the ferrogel.

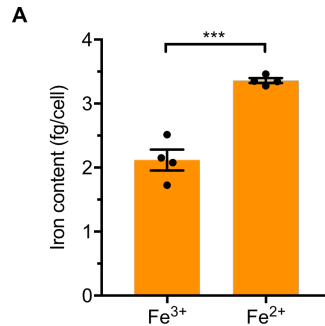


**Figure S8 | A.** Intracellular Iron content of UPMAE *E.coli* cultured in protein expression medium with either 1 mM Fe(III) or 1 mM Fe(II) as the iron source.

### Estimates of force in a magnetic separation column

The magnetic force on a cell with different magnetic susceptibility relative to surrounding medium is  $\vec{F}_m = \frac{V_{cell}\Delta\chi}{\mu_0}(B \cdot \nabla)B$  where  $V_{cell}$  is the cell volume,  $\Delta\chi$  is the bulk susceptibility difference between the cell and the medium,  $\mu_0$  is the permeability of free space,  $B$  is the magnetic field, and  $\nabla B$  is the magnetic field gradient. A MidiMACS separator produces a permanent field of  $B \approx 0.45$  T, and MACS LD columns produce field gradients of  $10^4$  T/m according to the manufacturer.<sup>[2,3]</sup> From our measurements of UPMAE cells,  $\Delta\chi \approx 4.8 \times 10^{-6}$  relative to water. This results in a magnetic force of  $F_m \approx 19.8$  fN. By comparison, the sedimentation force acting on a single *E.coli* cell is approximately  $\vec{F}_g = \frac{4}{3}\pi r_{cell}^3 g(\rho_{cell} - \rho_{fluid}) \approx 1.18$  fN, using  $r_{cell} = 0.65$   $\mu\text{m}$ , and where  $\rho_{fluid}$  is the density of water and  $\rho_{cell}$  is 1105 kg/m<sup>3</sup> [1].

## EXPERIMENTAL METHODS

### Preparation of cell culture for *in vitro* NMR and *in vivo* MRI.

The following culture media were used for all experiments with *E. coli*. All reagents, unless otherwise specified, were purchased from Millipore-Sigma.

**Table 1: Culture media used in experiments**

Media	Composition
Overnight growth	M9 base salts + 0.4% (w/v) Glucose + 0.2% (w/v) CAS + 2 mM MgCl <sub>2</sub> + 0.1 mM CaCl <sub>2</sub> + 10 μM 2,2-Bipyridyl
Protein expression	M9 base salts + 0.4% (w/v) Glucose + 0.2% (w/v) CAS + 2 mM MgCl <sub>2</sub> + 0.1 mM CaCl <sub>2</sub>
Cell maintenance	M9 base salts + 2 mM MgCl <sub>2</sub> + 0.1 mM CaCl <sub>2</sub>

Prior to all experiments, *E. coli* were freshly chemically transformed with 1 ng of plasmid DNA and grown to saturation overnight in growth medium containing 10 μM of 2-2 bipyridyl, in order to starve the cells of iron and thus trigger RhyB mediated silencing of endogenous ferritins<sup>[4]</sup>. Overnight cultures of Novagen BL21 R2 DE3 *E. coli* expressing UPMAG, as well as controls, were inoculated (1:100) into fresh protein expression medium (100mL in a 500 mL Erlenmeyer flask) and grown at 37°C with vigorous shaking at 250 RPM to OD 0.1, at which point IPTG and Fe(II) ammonium sulfate were added to final concentrations of 0.1 mM and 1 mM respectively. We found that the supplementation with Fe(II) led to more iron accumulation in cells than supplementation with Fe(III) (Supplementary Fig. S8). The temperature was then reduced to 30°C and cultures were grown for 36 hrs before harvest. Cultures were pelleted at 3500 g for 10 mins and subsequently resuspended in an equivalent culture volume of 1X PBS + 2 mM EDTA to wash away any extracellular iron. Cells were then pelleted at 3500 g for 10 mins and resuspended in 1/5 culture volume of cell maintenance medium. OD<sub>600</sub> was measured in a 1:100 dilution of the resuspended cultures, and all cultures were normalized to the same OD<sub>600</sub> by addition of cell maintenance medium. Subsequently, 0.3 mL PCR tubes with *E. coli* at a desired OD<sub>600</sub> were prepared by mixing stock suspensions with Optiprep, thus creating a uniformly suspended mixture. The total amount of Optiprep was kept constant across the different densities in order to ensure that the buffer relaxation rates were constant. PCR tubes were placed in a precast 1% agarose phantom to minimize magnetic susceptibility artifacts, and the phantom was subsequently imaged using a 7 Tesla horizontal bore Bruker MRI scanner. The same cell culture harvest and wash procedures were followed for preparing samples to be analyzed using a Bruker 500 MHz NMR spectrometer, with the only difference being that the total volume of sample analyzed was 0.8 mL. Data analysis for calculating relaxation rates was done using a custom Matlab script that fit mono-exponentials to the first 6 echoes in an echo train.

### Protein purification and concentration measurements

Novagen BL21 DE3 *E. coli* were freshly transformed with 1 ng of plasmid containing an N-terminal hexa-histidine (with TEV protease cleavage site)-tagged FLPM6A under a T7 promoter, and subsequently cultured in protein expression media (100 mL) containing 50 μg/ml kanamycin in a baffled flask at 37°C with constant shaking at 250 RPM. At OD<sub>600</sub> 0.1, cells were induced with 100 μM IPTG, either with or without supplementation of 1 mM ferrous ammonium sulfate. The temperature was lowered to 30°C to allow for protein expression for 36 hrs. 100 mL cultures of control *E. coli* expressing 6xHis-TEV-mRuby2 were likewise cultured in protein expression medium for downstream harvest and purification using Ni-NTA affinity chromatography. All cells were again harvested as previously described. Upon washing, cultures were centrifuged and frozen at -80°C for 1 hr prior to thawing at room temperature for 10 mins. Pellets were lysed with a cocktail of SoluLyse (1 mL SoluLyse/ 10 mL cell culture), protease-inhibitor EDTA free (1X), lysozyme (50 μg/ml), and DNase (10 μg/ml). Cells were lysed at 4°C overnight on a slow rotator and subsequently clarified by centrifugation at 16,000 g for 15 mins. The supernatant was then mixed with Ni-NTA superflow resin (1 ml resin/100 ml cell culture) and again incubated overnight at 4°C. Protein was purified using gravity flow Polyprep (Biorad) columns and eluted with 1M imidazole (pH 8.0). Proteins were then dialyzed into 1X PBS using spin filters (10 kDa cutoff), and protein concentration was measured using both Pierce 660 nm and Pierce BCA assay. The insoluble fraction in the clarified cell lysate was first diluted 10 fold (by volume) in a SoluLyse buffer containing 1% Triton X-100, 0.1% Tween 20, and 0.1% NP-40 and incubated overnight at 4°C on a rotator in order to completely solubilize all lipids. The mixture was subsequently centrifuged at 16,000g for 15 mins. The supernatant was decanted and the remaining dark pellet was resuspended in PBS containing 6M urea and sonicated for 2 mins (25% duty cycle, 35% amplitude). The mixture was then mixed with Ni-NTA superflow resin and the same procedure was followed as before for affinity purification with the exception that all wash and elution buffers contained 6M urea.

Protein purified from inclusion bodies when cells were grown in iron-poor media and protein purified from the soluble fraction when cells were grown in iron-rich media were both concentrated ~ 5 fold. All fractions (S.F. +/- Fe; I.B. +/- Fe) were mixed 1:1 with Laemmli buffer containing SDS, β-mercapatoethanol and 0.1 mM L-ascorbic acid, and boiled at 95°C for 10 mins prior to SDS-PAGE analysis (Supplementary Fig. S3A).

Intracellular iron to protein ratio was computed by taking a ratio of the measured intracellular iron concentrations with the measured soluble protein yield when cultures were grown in the absence of iron in the growth media. *E. coli* volume was set to 1.2 fl and a cell density of  $OD_{600,1} = 21.9 \pm 2.2 \times 10^8$  cfu/ml  $\cdot OD_{600}$  was used in all calculations, consistent with literature values. The saturation cell-culture density for UPMAG cultures grown in protein expression medium was measured to be  $OD_{600} = 6.5 \pm 0.8$ .

### SQUID Magnetometry and KappaBridge Susceptibility

Cells were grown and washed as described above. Washed cells were pelleted at 3500 g for 10 minutes in 50 mL sterile polypropylene tubes, and the supernatant was aspirated. The cell pellet was subsequently frozen at  $-80^{\circ}\text{C}$  for 1 hour, then lyophilized for 24 hours in order to completely remove any water. Care was taken to minimize dried pellet contact with any steel-containing materials, which are sources of ferromagnetic contaminants. The dried pellet was homogenized by vortexing. 10 – 15 mg of dried powder was placed in gelatin capsules, which were then analyzed using a SQUID MPMS (Quantum Design). All SQUID magnetization (field sweep) curves were acquired at 30 K. An empty capsule was also measured for reference. The data shown in the figures are the raw SQUID curves and do not include any background subtraction. The magnetization versus temperature data fit well to the Curie-Weiss law,  $\chi = \frac{C}{T-T_c}$ , as expected for purely paramagnetic materials. 80 – 120 mg of dried cell powder was also packed into acid-cleaned glass NMR tubes for susceptibility measurements using an Agico KappaBridge Susceptometer. The cell powder was packed into the tube such that it completely covered the probe's sensing volume, thus ensuring a homogeneous magnetic environment throughout the measurement process. The tube was purged with argon gas prior to measurements in order to remove any paramagnetic oxygen, and all measurements were done at  $19^{\circ}\text{C}$ . An empty glass tube was identically measured in order to obtain a reference susceptibility, which was then subtracted from all subsequent measurements to obtain the final bulk volume susceptibility.

To compute the maximum achievable volume susceptibility from an iron loaded cell, we first assumed that all iron atoms were high-spin ferric ions  $[\text{Fe}^{3+}]3d^5$ , with a spin of  $S = 5/2$ , using the Aufbau principle. The effective magnetic moment of a single ion is  $m_{\text{Fe}^{3+}} = g_e \mu_B \sqrt{S(S+1)}$ , where  $g_e$  is the Landé electronic g-factor and  $\mu_B$  is the Bohr magneton. Assuming ideal paramagnetic behavior, the bulk volume susceptibility follows the Curie law,  $\chi = \frac{\mu_0 N (m_{\text{Fe}^{3+}})^2}{3k_B T}$ , where  $N$  is the number of ferric ions per cubic meter within the cell (assuming a cell volume of 1.2 fl),  $\mu_0$  is vacuum permeability constant,  $k_B$  is the Boltzmann constant, and  $T$  is the temperature in Kelvin, which for our calculations was set to 293K (room temperature).

### Intracellular measurements of iron

Washed cells were concentrated to a final  $\text{OD}_{600}$  of 80. Serial dilutions were plated concomitantly with ferrozine measurements to get precise colony counts. 20  $\mu\text{L}$  of concentrated suspension was boiled in 180  $\mu\text{L}$  of trace-metal free grade pure nitric acid ( $\sim 70\%$ ) at  $56^{\circ}\text{C}$  for 6 hours to ensure complete dissolution of intracellular iron in a sterile 2 ml polypropylene Eppendorf tube. A blank tube containing 20  $\mu\text{L}$  of maintenance media was treated identically for reference. Ferrous ammonium sulfate hexahydrate standards (1  $\mu\text{g}/\text{ml}$  to 200  $\mu\text{g}/\text{ml}$ ) were also prepared and treated identically to be used for absorbance measurements. Boiled samples were serially diluted in sterile milliQ water. A previously described ferrozine assay was subsequently used to measure iron concentrations across the dilutions<sup>[5]</sup>. Iron content per cell was obtained by dividing the total iron measured by the colonies counted.

To measure the quantity of iron in the soluble and insoluble fractions respectively, 150 mL of BL21 DE3 *E. coli* expressing 6xHis-FLPM6A was cultured in protein expression media supplemented with 1 mM Fe(II). Washed cells were lysed with 10 mL of lysis buffer, as described above and the lysate was clarified by centrifugation. The insoluble fraction was resuspended in 10 mL of inclusion body lysis buffer containing 6M Urea. A ferrozine assay was performed using 20  $\mu\text{L}$  of both the soluble and resuspended insoluble fractions as described above. Iron contents were quantified per volume of the sample.

### In vitro MACS experiments

Washed bacteria were resuspended in M9 base media to a final  $\text{OD}_{600}$  of 0.5, then poured over a MACS LD column (Miltenyi Biotech), which was sandwiched between neodymium rare earth magnets ( $B_0 = 0.45 \text{ T}$ ). The column was then washed with degassed PBS containing 0.5% BSA, and trapped microbes were eluted with degassed M9 medium. Dilutions of the eluate were plated, and colonies were subsequently counted for both the eluate and wash fractions. Magnetic fields were simulated using Gmsn, a finite element simulator, using values for magnetic coercivity taken from K&J magnetics<sup>[6]</sup>. N52 NdFeB magnets (BX084BR) from K&J magnetics were used in the petri-dish magnetic capture experiments.

### In-vivo experiments with NU/J mice and BALB/cJ mice

Mouse experiments were conducted under a protocol approved by the California Institute of Technology's Institutional Animal Care and Use Committee. For *in vivo* imaging experiments, *E. coli* were once again prepared as before. Washed microbes were resuspended in cell-maintenance media to a final  $\text{OD}_{600}$  of 20. 100  $\mu\text{L}$  of microbes were then mixed with an equal volume of Matrigel at  $4^{\circ}\text{C}$  and immediately injected subcutaneously into the hind flanks of nude mice. Mice were allowed to rest for 15 mins in order to set the matrigel-bacteria mixture, then imaged using a Bruker 7 Tesla small animal scanner. An M2M Quadrature coil was used to excite and receive RF signals, and isofluorane anesthesia was kept at 1.5% for the duration of imaging. Body temperature was recorded using a rectal fiber optic probe and kept constant at  $37^{\circ}\text{C}$  using a PID controlled hot-air blower.

For gavage experiments, *E. coli* were cultured and washed as previously described. Bacteria were then resuspended in cell maintenance media to a final  $\text{OD}_{600}$  of 1. A mixture of FP and UPMAG expressing cells were prepared in a 10:1 ratio. 200  $\mu\text{L}$  of the mixture was then gavaged into female 8 weeks old BALB/cJ mice. Mice were then returned to cages with access to food and water. Feces was freshly collected and weighed from mice 3 – 4 hours after gavage and homogenized in cell-maintenance medium (50 mg/ml) using a bead beater. Fecal samples were subsequently clarified through a 75  $\mu\text{m}$  filter (BD Falcon) to remove large insoluble aggregates, then poured over 0.5% BSA-equilibrated MACS LD columns. Trapped microbes were eluted, and serial dilutions of the eluate were plated on LB Agar plates containing ampicillin (100  $\mu\text{g}/\text{ml}$ ) and IPTG (100  $\mu\text{M}$ ). Colonies were grown and allowed to express at  $30^{\circ}\text{C}$  for 36 hrs prior to imaging using a BioRad ChemiDoc gel imager. Fluorescence images were acquired using the Alexa546 filter set with exposure time fixed at 0.1 seconds. Colonies

(fluorescent and non-fluorescent) were counted manually and the enrichment ratio was calculated. A sub-sampling of 20 non-fluorescent colonies were sequenced to confirm their identity as carriers of the UPMAG plasmid.

### **In-vitro DLS experiments**

Purified 6xHis-FLPM6A was diluted to 100 µg/ml (~ 6.5 µM monomer) in PBS and then aerobically incubated with freshly prepared Fe(II) ammonium sulfate at molar ratios of 0, 8, 16, 32, 48, 64, 80, 160, and 320 at 37°C in sterile 2 ml polypropylene Eppendorf tubes (total reaction volume 300 µL in 100 mM HEPES, pH 7.0) for 1 hour. Control experiments consisted of Ni-NTA affinity purified 100 µg/ml of 6xHis-mRuby2 and free iron at the same concentrations. Photos were taken using a Google Pixel2 camera. 200 µL of each sample was used for the DLS measurement (Brookhaven Instruments) as per the manufacturer's protocol. Briefly, autocorrelation spectra were acquired for 10 seconds at 22 °C, and measurements were repeated with no dust filtering for 6 trials. Samples were mixed by pipetting between trials to avoid settling. Aliquots of the same samples were then mixed 1:1 with Native sample buffer (Bio-Rad) and loaded into a precast TGX gel (Bio-Rad), which was subsequently run at 80V for 70 mins. The gel was first treated with Prussian blue (Sigma) stain to visualize iron deposits and then treated with Coomassie blue stain (Thermo Fisher) to visualize protein.

### **Growth curves**

9 separate colonies of *E. coli* expressing either UPMAG or FP were picked and inoculated overnight in cell-growth media. Subsequently, cultures were diluted 1:100 with fresh protein expression medium containing both IPTG and/or Fe, and cultured in, square 96 well plates sealed with breathable tape (200 µL total volume) for 26 hrs at 30°C with maximum linear shaking. Growth curves were obtained by recording OD<sub>600</sub> every 7 minutes and subsequently fitted to the modified Gompertz equation to obtain growth rates and carrying capacities<sup>17</sup>.

### **Monte Carlo Simulations**

Nuclear spin relaxation was simulated using an adaptation of previously described code by randomly distributing spherical *E. coli* cells with  $\chi_V = +4.68$  ppm inside a 1000 µm<sup>3</sup> cubic simulation volume using periodic boundary conditions<sup>8,9</sup>. Cell radius was set to 0.65 µm to match previously reported equivalent cell volumes of *E. coli*<sup>10</sup>. The number of cells in the simulation volume was set to match the OD of our experimental data using the Agilent estimate of  $N_{\text{cells}} = \text{OD}_{600} \cdot V_{E.coli} \cdot 8 \times 10^{11}$ , where  $V$  is the simulation volume in cubic meters. The magnetic moment of each *E. coli* cell was calculated as  $m = \chi_V \cdot V \cdot H$  where  $\chi$  is the bulk magnetic susceptibility,  $V$  is the volume of the cell, and  $H$  is the bias field in the NMR spectrometer (11.7 Tesla). The magnetic field  $B$  in the extracellular space was explicitly calculated for each water molecule based on the sum contribution from each *E. coli* cell. 4032 water molecules were randomly assigned initial 3D spatial coordinates ( $\mathbf{r} = [x, y, z]$ ) in the simulation volume with phase  $\phi(t_0) = 0$  and allowed to diffuse according to previously established cellular diffusion models<sup>8,9</sup>. The phase in the rotating reference frame evolves according to  $\delta\phi(t) = -\gamma \cdot \mathbf{B}(\mathbf{r}) \cdot \delta t$  for water in the extracellular space, where  $\gamma$  is the proton gyromagnetic ratio and  $\mathbf{B}$  is the total magnetic field in the rotating reference frame as experienced by the water molecules. For water in the intracellular space, phase evolves according to  $\delta\phi(t) = \Delta\omega \cdot \delta t$ , where  $\Delta\omega$  is the shift in the Larmor frequency due to the difference in intracellular bulk magnetic susceptibility relative to external media. Re-focusing pulses were simulated by setting  $\phi(t) = -\phi(t - \delta t)$ . Cell membranes were modeled as semi-permeable boundaries with a permeability of  $2 \frac{\mu\text{m}}{\text{ms}}$ , in accordance with previously measured values for *E. coli* cells<sup>11</sup>. Intracellular and extracellular water diffusivity were set to 1 and  $2 \frac{\mu\text{m}^2}{\text{ms}}$  respectively, in accordance with previous studies of cellular diffusion and established values for water diffusivity at the temperature of our spectrometer bore (20 °C). Bulk spin magnetization in the sample was calculated as  $M(t) = \sum_i \cos[\phi_i(t)]$ , where  $i$  is the index of simulated water molecules and the magnetic moment of a single molecule is normalized to 1.  $T_2$  values were extracted from each simulated sample with a mono-exponential fit to the first 10 echoes. Background relaxation from buffer was accounted for by multiplying all simulated exponential decays with a mono exponential decay whose rate constant was equal to the experimentally measured relaxation rate of pure buffer.

We simulated three different diffusion models to determine the dominant relaxation mechanism for UPMAG expressing *E. coli*. In the combined model, both intracellular and extracellular contributions to relaxation were allowed as described above. In the "intracellular only" case, membrane permeability was as described above, but the  $\delta\phi$  for extracellular water was set to zero. In this way, we were able to isolate the intracellular relaxation that arises solely from water molecules transiting through a compartment with different magnetic susceptibility. In the "extracellular only" case, water molecules were initialized only in the extracellular space, and the cell membranes were modeled as impermeable to water. In this way, we were able to isolate the effect of the outer-sphere dipolar relaxation due to the net magnetic moment of the *E. coli* cells. All simulations were written in CUDA and performed on two NVIDIA K40 GPUs.

### **Mossbauer Spectroscopy**

Samples for Mössbauer measurements were prepared identically to those for magnetometry measurements. In brief, 100 ml of *E. coli* cultures expressing either UPMAG or BFR were grown in iron-rich media (1mM Fe(II)) and subsequently washed with PBS-EDTA to chelate any extracellular iron. Washed cell pellets were then snap frozen and lyophilized for 24 hours. 70 – 80 mg of dried cell powder was then placed in Teflon Mössbauer sample holders.

Mössbauer spectra were recorded on a spectrometer from SEE Co. (Edina, MN) operating in the constant acceleration mode in a transmission geometry. The sample was kept in an SVT-400 cryostat from Janis (Wilmington, MA). The quoted isomer shifts are relative to the centroid of the spectrum of a metallic foil of  $\alpha$ -Fe at room temperature (RT). Data were collected at 80 K with a 50 mT magnet applied parallel to the gamma rays. Data analysis was performed using version 4 of the program WMOSS ([www.wmoss.org](http://www.wmoss.org)) and quadrupole doublets were fit to Lorentzian lineshapes.

### Circular Dichroism Spectroscopy

300  $\mu$ l of 3.3  $\mu$ M of purified FLPM6A in 20 mM Tris pH 7 was loaded into quartz cells with a 1 mm optical path length for CD measurements at room temperature. CD spectra were recorded using an Aviv Model 430 CD spectrometer at room temperature between wavelengths of 190 – 300 nm and averaged across 4 measurements. A buffer blank consisting of 20 mM Tris pH 7 was likewise recorded in the same manner and subsequently subtracted from the spectrum with protein.

### Size-exclusion Chromatography

Ni-NTA affinity purified FLPM6A was desalted into PBS and loaded onto a Superdex-200 10/300 gel-chromatography column (GE Healthcare, Little Chalfont, UK) with a flow rate of 0.25 ml/min.

### Transmission Electron Microscopy

4  $\mu$ l of protein-iron mixtures were spotted onto carbon-coated copper grids that were pre-treated with glow-discharge for 2 mins and blotted with Whatman paper. For stained samples, 4  $\mu$ l of 2% Uranyl Acetate was added to the grids for 30 s before blotting. Grids were subsequently washed and rapidly blotted three times with 4  $\mu$ l of miliQ water to thoroughly remove any salts and residual stain and allowed to air-dry for 10 mins before imaging. For unstained samples, grids were washed and rapidly blotted three times with 4  $\mu$ l of miliQ water after sample was spotted and likewise allowed to air dry for 10 mins before imaging. All imaging was done using a 120 keV Tecnai T12 LaB6 TEM equipped with a Gatan Ultrascan 2k X 2k CCD.

### Western Blotting

FLPM6A was purified from the soluble fraction of crude cell lysates for cells grown either with or without 1 mM Fe(II) using Ni-NTA affinity purification (Qiagen). All samples, including the insoluble fractions, were mixed with Laemmli sample buffer (BioRad) and 2-mercaptoethanol (BioRad) and boiled at 56 C for 10 mins before being loaded onto BioRad Mini-TGX 4-20% Precast gels and run at 80V for 65 mins. The gel was then transferred onto nitrocellulose membrane using a Trans Blot Turbo cassette and blocked with 5% Milk in TBS-Tween for 1 hr at room temperature. The blot was subsequently incubated with Mouse anti hexa-histidine-HRP conjugate antibody (1:100, Santa Cruz Biotechnology) at room temperature for 6 hrs before being washed twice with TBS-Tween and subsequently developed for chemiluminescent imaging (BioRad).

### Statistical Analysis

Data were analyzed using GraphPad Prism version 7.0d for Mac. Unpaired parametric t-tests (two-tailed) were used throughout the manuscript. Asterisks indicate p-values below 0.05 (\*), 0.002 (\*\*), 0.0002 (\*\*\*) and 0.0001 (\*\*\*\*).

### Supplementary References:

- [1] N. G. Durmus, H. C. Tekin, S. Guven, K. Sridhar, A. Arslan Yildiz, G. Calibasi, I. Ghiran, R. W. Davis, L. M. Steinmetz, U. Demirci, *Proc. Natl. Acad. Sci.* **2015**, *112*, E3661–E3668.
- [2] C. C. Kim, E. B. Wilson, J. L. Derisi, *Malar. J.* **2010**, *9*, 1–5.
- [3] S. Miltenyi, W. Müller, W. Weichel, A. Radbruch, *Cytometry* **1990**, *11*, 231–8.
- [4] S. W. Seo, D. Kim, H. Latif, E. J. O'Brien, R. Szubin, B. O. Palsson, *Nat. Commun.* **2014**, *5*, 4910.
- [5] J. Riemer, H. H. Hoepken, H. Czerwinska, S. R. Robinson, R. Dringen, *Anal. Biochem.* **2004**, *331*, 370–5.
- [6] C. Geuzaine, J.-F. Rémacle, *Int. J. Numer. Methods Eng.* **2009**, *79*, 1309–1331.
- [7] M. H. Zwietering, I. Jongenburger, F. M. Rombouts, K. Van't Riet, *Appl. Environ. Microbiol.* **1990**, *56*, 1875–1881.
- [8] A. Mukherjee, D. Wu, H. C. Davis, M. G. Shapiro, *Nat. Commun.* **2016**, *7*, 1–9.
- [9] H. C. Davis, P. Ramesh, A. Bhatnagar, A. Lee-Gosselin, J. F. Barry, D. R. Glenn, R. L. Walsworth, M. G. Shapiro, *Nat. Commun.* **2018**, *9*, 1–9.
- [10] H. E. Kubitschek, J. A. Friske, *J. Bacteriol.* **1986**, *168*, 1466–1467.
- [11] E. Persson, B. Halle, *Proc. Natl. Acad. Sci. U. S. A.* **2008**, *105*, 6266–71.